Double-echo perfusion-weighted MR imaging: basic concepts and application in brain tumors for the assessment of tumor blood volume and vascular permeability

Abstract

Perfusion-weighted magnetic resonance (MR) imaging using contrast agents plays a key role in characterizing tumors of the brain. We have shown that double-echo perfusion-weighted MR imaging (DEPWI) is potentially useful in assessing brain tumors. Quantitative indices such as tumor blood volume are obtained using DEPWI, which allows correction of underestimation of tumor blood volume due to leakage of contrast agents from tumor vessels, in addition to simultaneous acquisition of tumor vessel permeability. This article describes basic concepts of DEPWI and demonstrates clinical applications in brain tumors.

Introduction

Recent advances in magnetic resonance (MR) techniques allow the assessment of tissue perfusion in various diseases of the central nervous system. The most widely applied method for measuring brain perfusion by MR imaging is referred to as the “dynamic susceptibility contrast technique” [1-4]. This approach uses the principles of indicator dilution methods, in which a decrease in T2 or T2* MR signal intensity is related to the passage of paramagnetic contrast agents through the capillary bed. Drops in MR signal intensity provide information about multiple hemodynamic parameters. In perfusion-weighted MR imaging (PWI), the term ”perfusion” is broadly applied to indicate several hemodynamic parameters including cerebral blood volume (CBV), cerebral blood flow and mean transit time, as derived from dynamic MR data. In brain tumors, tumor blood volume has been used for characterization of tumors [5-8].

Although single-echo PWI has played a key role in the assessment of tumor blood volume in clinical settings, this technique displays technical drawbacks in the assessment of brain tumors. Since tumors do not usually express the properties of an intact blood-brain barrier (BBB), T2* rate changes caused by intravascular contrast agents in brain tumors are usually contaminated by a T1 shortening effect due to leakage of contrast agent. Tumor blood volume as reported in previous studies using single-echo PWI is thus underestimated [9, 10].

We have proposed a new method, double-echo perfusion-weighted MR imaging (DEPWI), which can correct the underestimation of tumor blood volume and simultaneously provide information on the permeability of tumor vessels [11, 12]. The present article describes the basic concepts of DEPWI and demonstrates clinical applications of this technique in brain tumors.

Perfusion-Weighted MR Imaging in the Assessment of Tumor Blood Volume and Its Technical Drawbacks

PWI as referred to herein represents a single-echo dynamic susceptibility contrast MR technique, and relies on T2 or T2* shortening effects due to the first pass of contrast agent [1-4]. Unlike conventional MR imaging, the basis of PWI does not rely on relaxivity (dipole-dipole) effects, instead primarily relying on magnetic susceptibility effects. T2 and T2*-weighted dynamic susceptibility contrast MR imaging takes advantage of the compartmentalization of contrast agent in capillaries. Magnetic susceptibility effects act on a longer range than previously described dipole-dipole interactions, extending outside vessels for a distance roughly equal to the radius of the blood vessel. This indicates that these effects are not just limited to the blood pool, but involve the entire brain. The measured MR signal intensity change versus time curve is converted into a contrast agent tissue concentration ($\Delta R2$ or $\Delta R2^*$) versus time curve. This relationship is the key link allowing the calculation of cerebral hemodynamics. Since the signal drop is directly related to the concentration of intravascular gadolinium, tumor blood volume can be calculated if the amount of gadolinium is known. Tumor blood volume is calculated from the area under the T2 or T2* rate change ($\Delta R2$ or $\Delta R2^*$), and $\Delta R2$ ($\Delta R2^*$) can be calculated from signal intensity before and during the passage of contrast agent, as follows:

$$\Delta R2\ (\Delta R2^*) = -\ln [S(t) / S(0)]/ TE \qquad [1],$$

where S(t) is MR signal at time (t), S(0) is the mean MR signal before the arrival of contrast agent, and TE is echo time. Tumor blood volume can be normalized by volume of the reference tissue (e.g., white matter) to generate an index of tumor vascularity.

The tumor blood volume obtained by this equation is essentially based on the assumption that the BBB is intact and able to keep the contrast agent within the vascular system. However, the BBB is usually disrupted in brain tumors, and contrast agent leaks into the tumor interstitium. This reduction of the compartmentalization decreases local field inhomogeneities. In addition, extravascular contrast agents cause a local T1 shortening. These two factors hinder the proper calculation of tumor blood volume, resulting in an underestimation of tumor blood volume. Some investigators have reported that post-processing algorithms can compensate for moderate degrees of BBB disruption [13]. Alternatively, a small dose of gadolinium may reduce T1 shortening to some degree during the first pass of the dynamic study [7]. We have shown that the DEPWI can correct such T1 shortening effects in the assessment of brain tumors [9, 11].

Principles of Double-Echo Perfusion-Weighted MR Imaging

After bolus injection, gadopentetate dimeglumine causes a T2* rate change (ΔR2*) in brain tumors. This change is contaminated by a T1-shortening effect due to leakage of contrast material [7, 14]. Miyati et al. [15] evaluated tumor vascularity while correcting for T1 shortening by using double-echo MR imaging. R2* is:

$$R2^* = \ln [S(TE_1)/S(TE_2)]/ (TE_2-TE_1) \quad [2],$$

where R2* is the T2* rate (1/T2*), and $S(TE_1)$ and $S(TE_2)$ represent the signal of the first and second TE, respectively. Consequently, ΔR2* with correction to T1 shortening ($\Delta R2^*_{T1C}$) is:

$$\Delta R2^*_{T1C} = R2^* - R2^*_0 \quad [3],$$

where $R2^*_0$ is the mean T2* rate before the arrival of contrast agent.

Tumor blood volume can be estimated on the basis of the T2* shortening effect of intravascular contrast material using the following equation, fitted with gamma function ($\Delta R2^*_{T1Cf}$) to eliminate the second-pass effect:

$$\text{tumor blood volume} = \int_0^\infty \Delta R2^*_{T1Cf}(t)dt \quad [4],$$

where t is time.

After bolus injection, contrast agent is extracted from the intravascular space to the extravascular space. With a simple two-compartment model, assuming no back diffusion and no recirculation effect, extraction fraction (E) of the contrast agent is:

$$E = \frac{C_T}{F \cdot \int_0^\infty C_A(t)\,dt} \quad [5],$$

where C_T represents the concentration of contrast agent in the extravascular space of the tissue (a constant after the first pass ends), F represents regional blood flow, and $C_A(t)$ represents the arterial input function. As MR imaging cannot directly quantify the concentration of contrast agent in the intra- or extravascular space or absolute blood volume, E cannot be directly calculated. However, Equation 5 gives a clue regarding how to generate useful indices for vascular permeability.

As concentration of contrast agent in the extravascular space of the tissue, (C_T), displays a linear relationship with $\Delta R2^*_{T1C}(t)$ - $\Delta R2^*_{T1U}(t)(t > t_0)$ [11], the latter can be used

as a parameter of contrast material leakage to the extravascular space. The T1-uncorrected $\Delta R2^*$ calculated from the single-echo MR data (from Equation 1) is denoted as $\Delta R2^*_{T1U}$:

$$LV = \Delta R2^*_{T1C}(t) - \Delta R2^*_{T1U}(t) \quad [6],$$

where LV is the leakage value and t is time. Note that the leakage value reflects the total amount of leaked contrast agent, not the permeability or extraction fraction itself. As $\Delta R2^*_{T1Cf}$ max is known to be proportional to tumor blood flow [16], Equation 5 can be re-described as follows:

$$E = \frac{C_T}{F \cdot \int_0^\infty C_A(t)\,dt} = \frac{\Delta R2^*_{T1C}(t) - \Delta R2^*_{T1U}(t)}{\Delta R2^*_{T1Cf}\,\max \cdot \int_0^\infty C_A(t)\,dt} \quad [7],$$

where $\Delta R2^*_{T1Cf}$ max represents the maximum height of the curve $\Delta R2^*_{T1C}$. If we can assume that variation in arterial input function among subjects is negligible, Equation 7 can be further simplified as follows:

$$E = \frac{C_T}{F \cdot \int_0^\infty C_A(t)\,dt} \propto \frac{\Delta R2^*_{T1C}(t) - \Delta R2^*_{T1U}(t)}{\Delta R2^*_{T1Cf}\,\max} \quad [8],$$

and

$$LI = \frac{\Delta R2^{*}_{T1C}(t) - \Delta R2^{*}_{T1U}(t)}{\Delta R2^{*}_{T1Cf}max} \quad [9],$$

where leakage index (LI) may in part reflect tissue extraction fraction (E). Details of this have been documented in the literature [11].

The Advantage and Drawback of Double-Echo Perfusion-Weighted MR Imaging

The quantification of cerebral perfusion using dynamic susceptibility contrast MR imaging is theoretically based on the assumption of an intact BBB. However, after an intravenous bolus injection, there is prompt distribution of the contrast agent through the intravascular and extracellular spaces of the brain tumor. The contrast agent causes T1 shortening effect once it has reached the interstitial space, resulting in underestimation of the blood volume of brain tumors. On the other hand, double-echo perfusion-weighted MR imaging (DEPWI) can correct the tissue response function of brain tumors having no BBB, making it possible to correctly estimate the blood volume of brain tumors that have no BBB. This is a distinct advantage of DEPWI.

The quantification of the extravasation of the contrast agent in the tissue during bolus passage is based on a simple two-compartment kinetic model. This method separates the intravascular response from the extravascular component. Although diffusion of the contrast agent from the vessels to the interstitial space (K_1) is taken into account in our method, back-diffusion from the interstitial space into the vessels (k_2) is not taken into account, which may cause underestimation of the tissue extraction fraction (E). This is a drawback of DEPWI.

MR Imaging Techniques

For DEPWI, we used two echoes with TEs of 7 ms and 23 ms, a spoiled gradient-recalled acquisition in steady state (SPGR) sequence (TR/TE: 33.3/7 or 23 ms; flip angle, 10°; 0.75 signal acquired; matrix, 256 × 128; section thickness, 7 mm; and a rectangular field of view, 24 × 16 cm). Dynamic images were obtained at the level of a single section corresponding to the level of the most appropriate abnormalities seen on non-enhanced MR imaging in patients with brain tumors. After 5 images were acquired, gadopentetate dimeglumine (0.1 mmol/kg body weight) was rapidly injected intravenously at a rate of 5 mL/s using an MR-compatible power injector, followed by a 20-mL saline solution flush. After administration of the gadopentetate dimeglumine bolus, a dynamic series of 50 sets of double-echo images were obtained at 2.4-s intervals. For this sequence, total acquisition time was approximately 2 min. One drawback of the double-echo SPGR sequence is the single-slice acquisition. Echo-planar imaging would have been desirable for multi-slice acquisition [17, 18].

Data Analysis

Regions of interest were placed on both normal white matter and solid portions of tumor. Time series of signal intensity were converted to changes in $\Delta R2^*_{T1C}$ and $\Delta R2^*_{T1U}$ (see above). Gamma fitting of $\Delta R2^*_{T1C}$ data was performed to generate $\Delta R2^*_{T1Cf}$. Index of tumor blood volume was calculated using the tumor blood volume normalized by CBV of the white matter (vascularity index). To obtain the leakage value, ($\Delta R2^*_{T1C}$ - $\Delta R2^*_{T1U}$) values immediately after the first pass of the time-to-$\Delta R2^*_{T1Cf}$ curve were averaged (Fig. 1).

Clinical Application of DEPWI in Brain Tumors

We have applied the DEPWI technique for brain tumors including meningiomas, neurinomas and gliomas [9, 11, 12], in which strong contrast enhancement was shown due to disrupted or absent BBB. Using DEPWI, quantitative indices such as tumor blood volume and leakage indices are obtained to characterize tumor tissues.

Meningiomas and neurinomas are extra-axial brain tumors that have no BBB. These tumors occasionally originate in similar locations, such as the cerebellopontine angle and skull base. Tumor blood volume is significantly greater in meningioma than in neurinoma on single-echo PWI [6], even with contamination of the T1-shortening effect caused by contrast agent leaking into the extravascular space. DEPWI verifies the greater tumor blood volume in meningioma compared to neurinoma [11]. Conversely, leakage index is significantly higher in neurinoma than in meningioma. As shown in Figure 2, the typical meningioma is characterized by high tumor blood volume and low leakage index. The typical neurinoma, on the other hand, is characterized by large leakage index but a tumor blood volume similar to that of normal white matter (Fig. 3). We applied both tumor blood volume and leakage index to characterize 22 brain tumors (meningioma, n=11; neurinoma, n=11). Tumor characteristics are summarized in Figure 4. Substantial overlap exists in tumor blood volume (vascularity index), while the leakage index appears to display better separation for the two types of neoplasm [11].

The higher leakage index in neurinoma may suggest that these tumors are more permeable to contrast agent in tumor vessels than meningiomas are [19]. According to previous studies [20], the endothelial fenestration and open-gap junctions that are commonly found in the capillaries of neurinomas and meningiomas function as routes into the extravascular space, where the T1 effect of gadolinium can be achieved. Capillary structures in neurinoma are simple, and gap junctions are usually short, straight and patent [20], freely

communicating with extravascular space. In meningioma, on the other hand, gap junctions are often tortuous, elongated and sinusoidal, and frequently link with abnormal endothelial cells similar to tumor cells [20]. Differences in gap junctions between the two tumor types may explain why, during first transit, contrast agent achieves greater and faster access into the extravascular space in neurinoma, causing larger leakage indices in neurinoma than in meningioma.

PWI has recently been used to evaluate the vascularity of gliomas [21], focusing on grading of gliomas [21], stereotactic biopsy guidance [8], assessment of response to therapy [22-29] and differentiation of therapy-induced necrosis and recurrent tumor [30], as degree of vascular proliferation represents an important parameter in determining biological aggressiveness and histopathological grading of astrocytoma [31, 32]. However, as mentioned above, single-echo PWI techniques intrinsically underestimate tumor blood volume in high-grade glioma due to BBB disruption, which may lead to erroneous interpretations and flawed treatment strategies. We evaluated tumor blood volume in glioblastoma multiforme (GBM) using DEPWI and compared tumor blood volumes with and without T1 shortening correction [9]. Tumor blood volumes were approximately 1.8-fold higher with T1 correction than without T1 correction. Differences in tumor blood volume were visually apparent between parametric maps with and without T1 correction (Fig. 5). Careful attention should thus be paid to the underestimation of tumor blood volume resulting from T1 shortening effects when using single-echo PWI. DEPWI may be more suitable for analyzing blood volume in high-grade astrocytoma, particularly when determining treatment strategy.

Information regarding vascular permeability of astrocytoma may further characterize this neoplasm. In our preliminary study [12], tumor blood volume was much higher in GBM than in pilocytic astrocytoma, while pilocytic astrocytoma showed much higher leakage index than GBM (Figs. 6, 7). These results may indicate that GBM is characterized by high tumor

blood volume, while pilocytic astrocytoma displays characteristic high vascular permeability. In general, differentiating between GBM and pilocytic astrocytoma is easy using conventional MR imaging, but vascular density and leakage can be investigated utilizing the present MR methods.

Glioma grading is extremely important in a clinical setting because high-grade gliomas are usually treated by intensive methods such as adjuvant radiation therapy and chemotherapy after resection, while low-grade gliomas are not. Currently, tumor grading is based on histopathologic assessment; however, this has limitations, including potential sampling error associated with the limited number of biopsy samples. Even with surgery, histology can be performed only on an excised tumor, and residual tumor tissue cannot be examined. Therefore, information regarding tumor blood volume and vascular permeability can be useful in determining appropriate treatment strategies for gliomas. In the near future, investigations will determine whether DEPWI can classify glioma into proper grades using combined parameters of tumor blood volume and vascular permeability.

Conclusion

Single-echo PWI is currently in wide use for assessing brain tumors. DEPWI can correct the T1 shortening effect resulting from leakage of contrast agent, allowing compensation for underestimation of tumor blood volume. Furthermore, information on vascular permeability is simultaneously available using this method. This method thus appears to provide additional useful information about brain tumors.

Acknowledgements

The authors wish to thank Yoshiyuki Ishimori, R.T., of the University of Fukui, Genji Asanuma, R.T., of Mie University, and Tsuyoshi Matsuda, R.T., of GE-Yokogawa Medical Systems for their technical support.

References

1. Villringer A, Rosen BR, Belliveau JW, Ackerman JL, Lauffer RB, Buxton RB, Chao YS, Wedeen VJ, Brady TJ (1988) Dynamic imaging with lanthanide chelates in normal brain: contrast due to magnetic susceptibility effects. Magn Reson Med 6: 164-174.
2. Rosen BR, Belliveau JW, Buchbinder BR, McKinstry RC, Porkka LM, Kennedy DN, Neuder MS, Fisel CR, Aronen HJ, Kwong KK, et al. (1991) Contrast agents and cerebral hemodynamics. Magn Reson Med 19: 285-292.
3. Rosen BR, Belliveau JW, Aronen HJ, Kennedy D, Buchbinder BR, Fischman A, Gruber M, Glas J, Weisskoff RM, Cohen MS, et al. (1991) Susceptibility contrast imaging of cerebral blood volume: human experience. Magn Reson Med 22: 293-299; discussion 300-293.
4. Edelman RR, Mattle HP, Atkinson DJ, Hill T, Finn JP, Mayman C, Ronthal M, Hoogewoud HM, Kleefield J (1990) Cerebral blood flow: assessment with dynamic contrast-enhanced T2*-weighted MR imaging at 1.5 T. Radiology 176: 211-220.
5. Maeda M, Itoh S, Kimura H, Iwasaki T, Hayashi N, Yamamoto K, Ishii Y, Kubota T (1993) Tumor vascularity in the brain: evaluation with dynamic susceptibility-contrast MR imaging. Radiology 189: 233-238.
6. Maeda M, Itoh S, Kimura H, Iwasaki T, Hayashi N, Yamamoto K, Ishii Y, Kubota T (1994) Vascularity of meningiomas and neuromas: assessment with dynamic susceptibility-contrast MR imaging. AJR Am J Roentgenol 163: 181-186.
7. Aronen HJ, Gazit IE, Louis DN, Buchbinder BR, Pardo FS, Weisskoff RM, Harsh GR, Cosgrove GR, Halpern EF, Hochberg FH, Rosen BR (1994) Cerebral blood volume maps of gliomas: comparison with tumor grade and histologic findings. Radiology 191: 41-51.

8. Knopp EA, Cha S, Johnson G, Mazumdar A, Golfinos JG, Zagzag D, Miller DC, Kelly PJ, Kricheff, II (1999) Glial neoplasms: dynamic contrast-enhanced T2*-weighted MR imaging. Radiology 211: 791-798.

9. Uematsu H, Maeda M, Sadato N, Matsuda T, Ishimori Y, Koshimoto Y, Kimura H, Yamada H, Kawamura Y, Yonekura Y, Itoh H (2001) Blood volume of gliomas determined by double-echo dynamic perfusion- weighted MR imaging: a preliminary study. AJNR Am J Neuroradiol 22: 1915-1919.

10. Essig M, Wenz F, Scholdei R, Bruning R, Berchtenbreiter C, Meurer M, Knopp MV (2002) Dynamic susceptibility contrast-enhanced echo-planar imaging of cerebral gliomas. Effect of contrast medium extravasation. Acta Radiol 43: 354-359.

11. Uematsu H, Maeda M, Sadato N, Matsuda T, Ishimori Y, Koshimoto Y, Yamada H, Kimura H, Kawamura Y, Hayashi N, Yonekura Y, Ishii Y (2000) Vascular permeability: quantitative measurement with double-echo dynamic MR imaging--theory and clinical application. Radiology 214: 912-917.

12. Uematsu H, Maeda M, Sadato N, Ishimori Y, Matsuda T, Koshimoto Y, Kimura H, Yamada H, Kawamura Y, Takeuchi H, Yonekura Y, Itoh H (2002) Measurement of the vascularity and vascular leakage of gliomas by double-echo dynamic magnetic resonance imaging: a preliminary study. Invest Radiol 37: 571-576.

13. Weisskoff RM, Boxerman JL, Sorensen AG, Kulke SM, Campbell TA, Rosen BR (1994) Simultaneous blood volume and permeability mapping using a single Gd-based contrast injection. Proceedings of the 2nd SMR meeting 279.

14. Bruening R, Kwong KK, Vevea MJ, Hochberg FH, Cher L, Harsh GR 4th, Niemi PT, Weisskoff RM, Rosen BR (1996) Echo-planar MR determination of relative cerebral blood volume in human brain tumors: T1 versus T2 weighting. AJNR Am J Neuroradiol 17: 831-840.

15. Miyati T, Banno T, Mase M, Kasai H, Shundo H, Imazawa M, Ohba S (1997) Dual dynamic contrast-enhanced MR imaging. J Magn Reson Imaging 7: 230-235.

16. Muramoto S, Uematsu H, Sadato N, Tsuchida T, Matsuda T, Hatabu H, Yonekura Y, Itoh H (2002) H(2) (15)0 positron emission tomography validation of semiquantitative prostate blood flow determined by double-echo dynamic MRI: a preliminary study. J Comput Assist Tomogr 26: 510-514.

17. Vonken EJ, van Osch MJ, Bakker CJ, Viergever MA (1999) Measurement of cerebral perfusion with dual-echo multi-slice quantitative dynamic susceptibility contrast MRI. J Magn Reson Imaging 10: 109-117.

18. Vonken EP, van Osch MJ, Bakker CJ, Viergever MA (2000) Simultaneous quantitative cerebral perfusion and Gd-DTPA extravasation measurement with dual-echo dynamic susceptibility contrast MRI. Magn Reson Med 43: 820-827.

19. Watabe T,Azuma T (1989) T1 and T2 measurements of meningiomas and neuromas before and after Gd-DTPA. AJNR Am J Neuroradiol 10: 463-470.

20. Long DM (1973) Vascular ultrastructure in human meningiomas and schwannomas. J Neurosurg 38: 409-419.

21. Sugahara T, Korogi Y, Kochi M, Ikushima I, Hirai T, Okuda T, Shigematsu Y, Liang L, Ge Y, Ushio Y, Takahashi M (1998) Correlation of MR imaging-determined cerebral blood volume maps with histologic and angiographic determination of vascularity of gliomas. AJR Am J Roentgenol 171: 1479-1486.

22. Pardo FS, Aronen HJ, Kennedy D, Moulton G, Paiva K, Okunieff P, Schmidt EV, Hochberg FH, Harsh GR, Fischman AJ, et al. (1994) Functional cerebral imaging in the evaluation and radiotherapeutic treatment planning of patients with malignant glioma. Int J Radiat Oncol Biol Phys 30: 663-669.

23. Wenz F, Rempp K, Hess T, Debus J, Brix G, Engenhart R, Knopp MV, van Kaick G, Wannenmacher M (1996) Effect of radiation on blood volume in low-grade astrocytomas and normal brain tissue: quantification with dynamic susceptibility contrast MR imaging. AJR Am J Roentgenol 166: 187-193.

24. Tomoi M, Maeda M, Yoshida M, Yamada H, Kawamura Y, Hayashi N, Ishii Y, Kubota T (1999) Assessment of radiotherapeutic effect on brain tumors by dynamic susceptibility contrast MR imaging: a preliminary report. Radiat Med 17: 195-199.

25. Sugahara T, Korogi Y, Tomiguchi S, Shigematsu Y, Ikushima I, Kira T, Liang L, Ushio Y, Takahashi M (2000) Posttherapeutic intraaxial brain tumor: the value of perfusion-sensitive contrast-enhanced MR imaging for differentiating tumor recurrence from nonneoplastic contrast-enhancing tissue. AJNR Am J Neuroradiol 21: 901-909.

26. Essig M, Waschkies M, Wenz F, Debus J, Hentrich HR, Knopp MV (2003) Assessment of brain metastases with dynamic susceptibility-weighted contrast-enhanced MR imaging: initial results. Radiology 228: 193-199.

27. Fuss M, Wenz F, Scholdei R, Essig M, Debus J, Knopp MV, Wannenmacher M (2000) Radiation-induced regional cerebral blood volume (rCBV) changes in normal brain and low-grade astrocytomas: quantification and time and dose-dependent occurrence. Int J Radiat Oncol Biol Phys 48: 53-58.

28. Fuss M, Wenz F, Essig M, Muenter M, Debus J, Herman TS, Wannenmacher M (2001) Tumor angiogenesis of low-grade astrocytomas measured by dynamic susceptibility contrast-enhanced MRI (DSC-MRI) is predictive of local tumor control after radiation therapy. Int J Radiat Oncol Biol Phys 51: 478-482.

29. Weber MA, Thilmann C, Lichy MP, Gunther M, Delorme S, Zuna I, Bongers A, Schad LR, Debus J, Kauczor HU, Essig M, Schlemmer HP (2004) Assessment of

irradiated brain metastases by means of arterial spin-labeling and dynamic susceptibility-weighted contrast-enhanced perfusion MRI: initial results. Invest Radiol 39: 277-287.

30. Cha S, Knopp EA, Johnson G, Wetzel SG, Litt AW, Zagzag D (2002) Intracranial mass lesions: dynamic contrast-enhanced susceptibility-weighted echo-planar perfusion MR imaging. Radiology 223: 11-29.

31. Zagzag D, Friedlander DR, Dosik J, Chikramane S, Chan W, Greco MA, Allen JC, Dorovini-Zis K, Grumet M (1996) Tenascin-C expression by angiogenic vessels in human astrocytomas and by human brain endothelial cells in vitro. Cancer Res 56: 182-189.

32. Leon SP, Folkerth RD, Black PM (1996) Microvessel density is a prognostic indicator for patients with astroglial brain tumors. Cancer 77: 362-372.

Figure Legends

Figure 1. Time-concentration curve of GBM computed from double-echo SPGR sequence. The time-concentration curve calculated from double-echo MR data ($\Delta R2^*_{T1C}$) is represented by closed circles (●), the gamma-fitted curve ($\Delta R2^*_{T1cf}$) is represented by a bold line, and the time-concentration curve calculated from second echo MR data ($\Delta R2^*_{T1U}$) is represented by open circles (○). Note that $\Delta R2^*_{T1U}$ is underestimated by the T1 shortening effect. The gamma-fitted time-concentration curve of normal white matter is represented by a fine line. Leakage values were plotted using open triangles. To obtain leakage value, ($\Delta R2^*_{T1C}$ - $\Delta R2^*_{T1U}$) values immediately after the first pass of time-to-$\Delta R2^*_{T1Cf}$ curve were averaged.

Figure 2. Meningioma case

Contrast-enhanced T1-weighted spin-echo MR image (left), blood volume map (middle) and leakage value map (right). Tentorial meningioma shows intense contrast enhancement on the left image (white arrow). Note the high vascularity and low leakage of the meningioma.

Figure 3. Neurinoma case

Contrast-enhanced T1-weighted spin-echo image (left), blood volume map (middle) and leakage value map (right). Neurinoma shows intense contrast enhancement in the right cerebello-pontine angle on the left image (white arrow). Note the low blood volume and relatively high leakage value of the neurinoma.

Figure 4. Semi-logarithmic plot of leakage index and vascularity index for meningioma (○, n=11) and neurinoma (■, n=11). Substantial overlap in vascularity index existed between the two tumor types. Leakage index separated tumors in all except one case.

Figure 5. GBM case

Contrast-enhanced T1-weighted spin-echo image (left), blood volume map without T1 shortening correction (middle) and blood volume map (T1 shortening compensated by double-echo SPGR sequence) (right). In this case, the histologic diagnosis was verified as GBM by means of surgical resection. T1-weighted spin echo image and parametric images are at slightly different angles. GBM is recognized as a strongly enhancing tumor in the right occipital lobe. Note that GBM displays larger blood volume when T1 shortening correction is performed using the double-echo sequence (white arrow). Actual blood volume was 1.5-fold higher than blood volume without T1 shortening correction.

Figure 6. GBM case

Contrast-enhanced T1-weighted spin-echo image (left), blood volume map (middle) and leakage value map (right). GBM shows inhomogeneous enhancement in the right fronto-parietal lobe. Note high blood volume and relatively low leakage value of the tumor.

Figure 7. Pilocytic astrocytoma case

Contrast-enhanced T1-weighted spin-echo image (left), blood volume map (middle) and leakage value map (right). T1-weighted spin echo image and parametric images are at slightly different angles. The pilocytic astrocytoma shows intense homogeneous enhancement in the solid portion of tumor on the left image (white arrow). Note the low blood volume and high leakage value of the tumor.

Fig.1

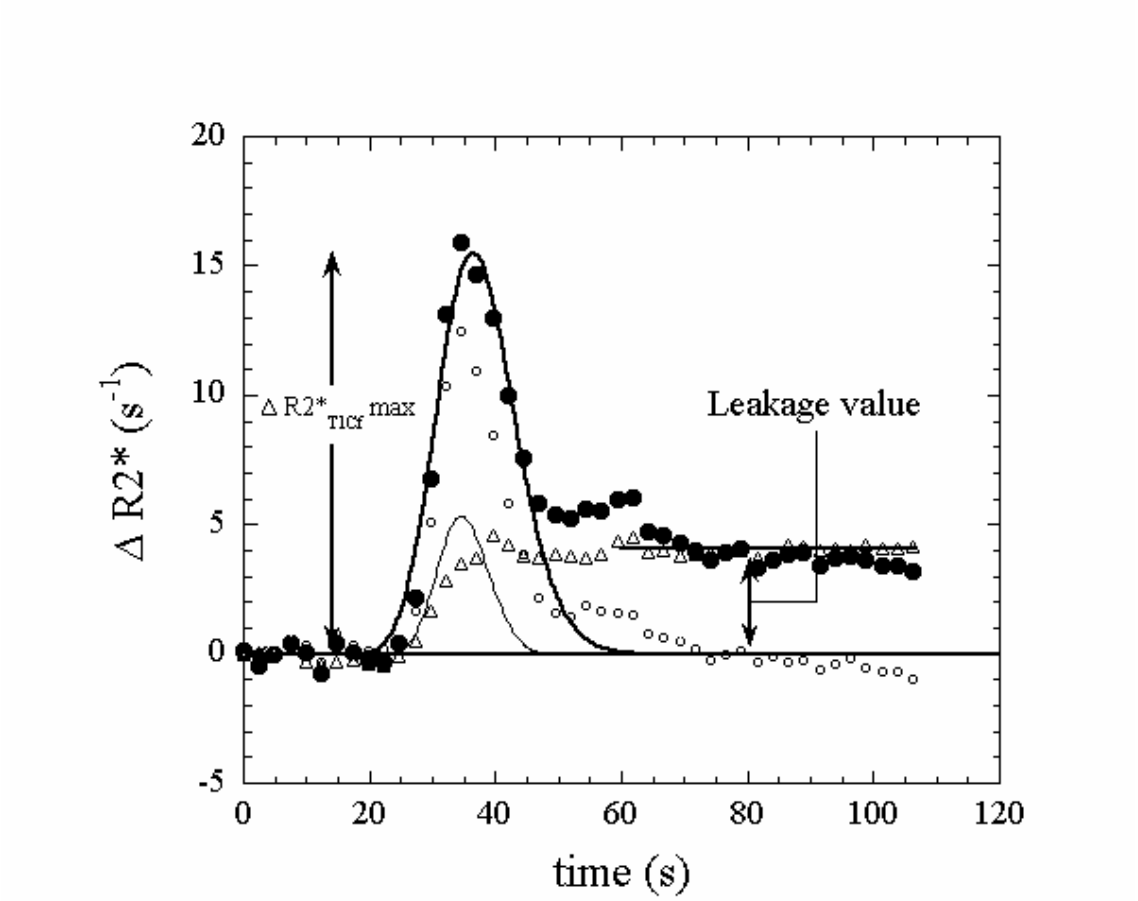
20
15
10
5
0
-5
0
20
40
60
80
100
120
time (s)
Δ R2* (s-1)
Δ R2*TICI max
Leakage value

Fig.2

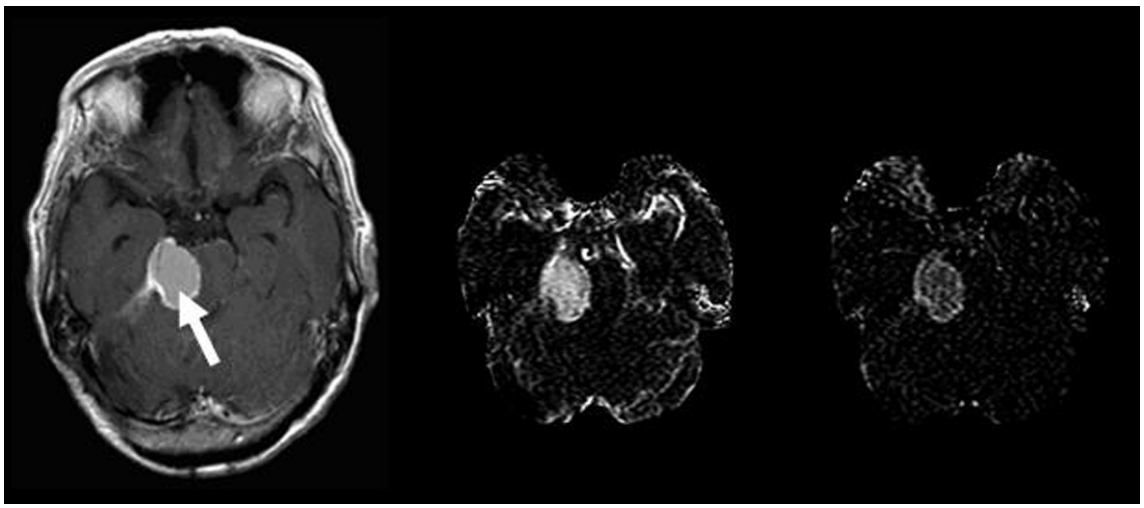

Fig.3

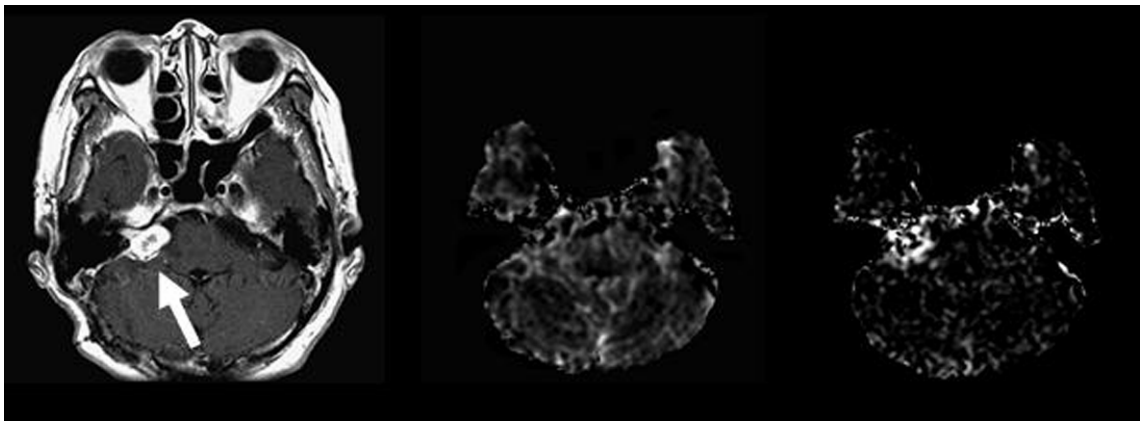

Fig.4

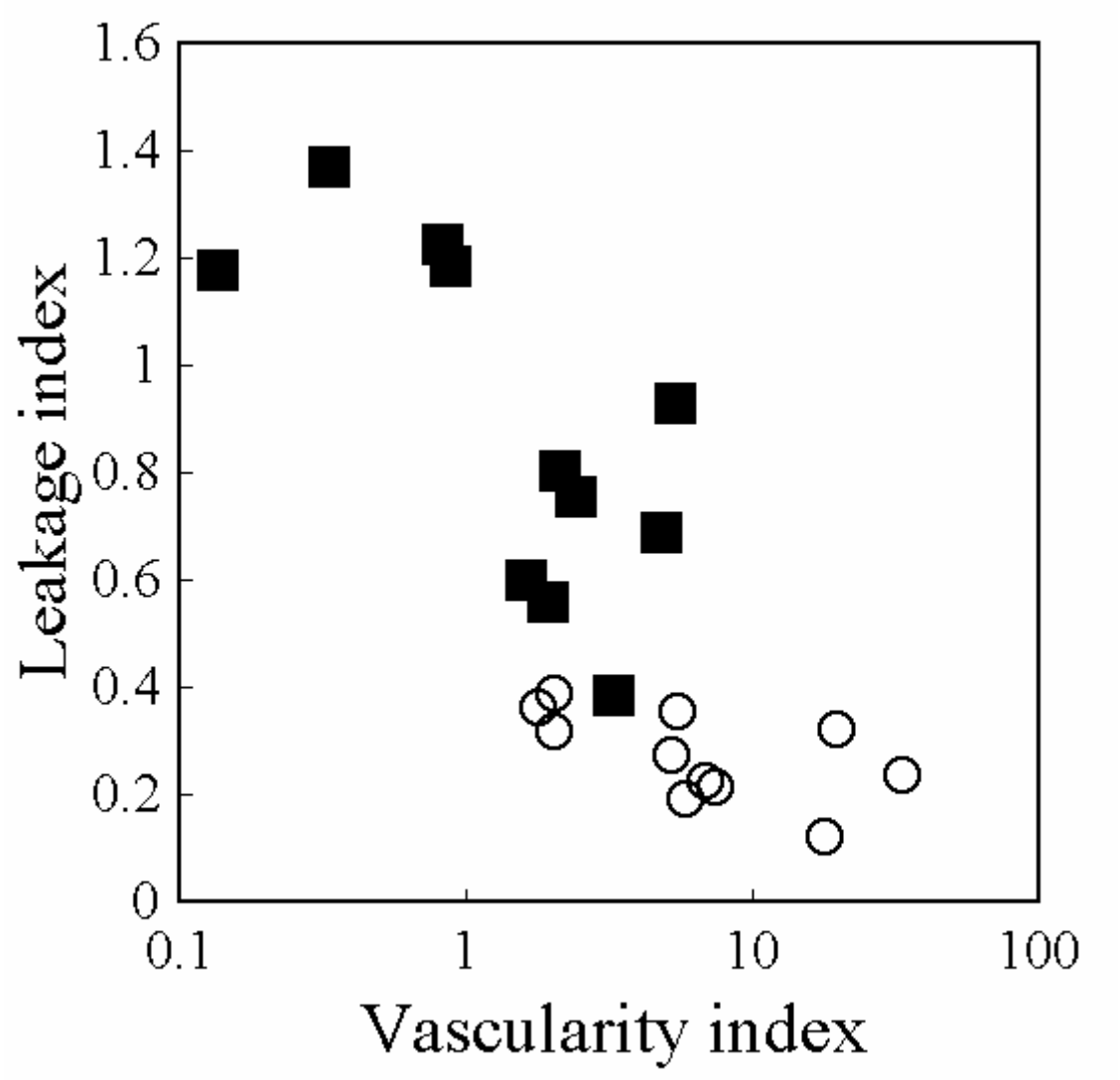
Leakage index
1.6
1.4
1.2
1
0.8
0.6
0.4
0.2
0
0.1
1
10
100
Vascularity index

Fig.5

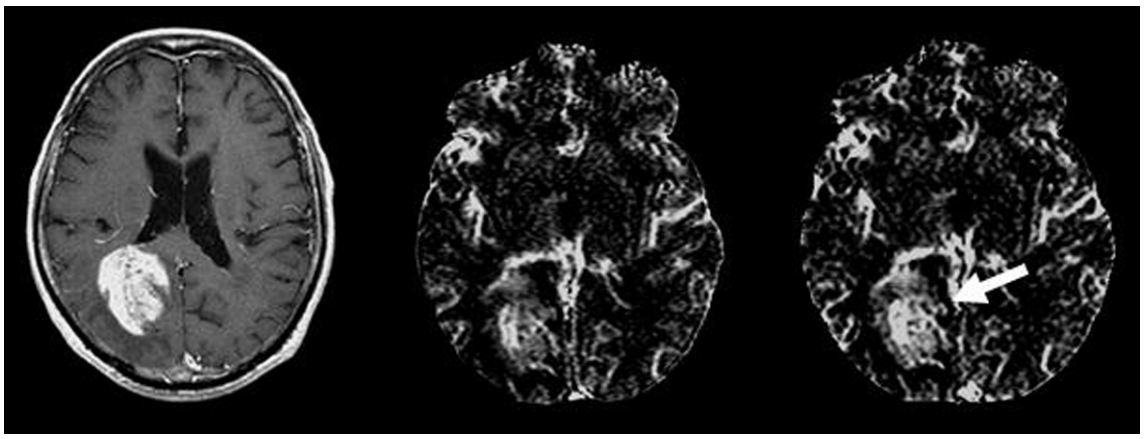

Fig.6

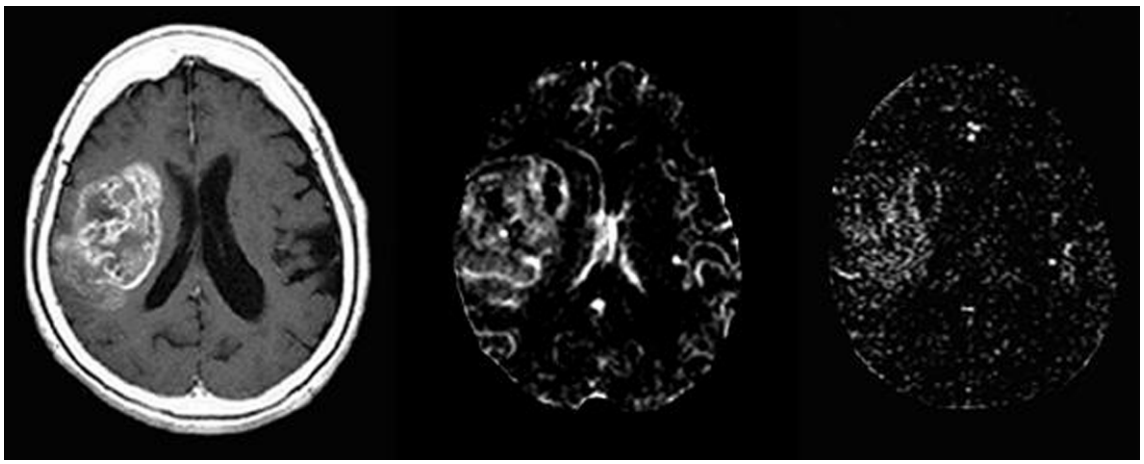

Fig.7